This is a preprint, the final version is subject to change, of the American Mineralogist (MSA)
Cite as Authors (Year) Title. American Mineralogist, in press.
DOI: https://doi.org/10.2138/am-2020-7363

REVISION 1

New IR spectroscopic data for determination of water abundances in hydrous pantelleritic glasses

Paola Stabile[1,*], Ernestina Appiah[1], Marco Bello[1], Gabriele Giuli[1], Eleonora Paris[1], and Michael R. Carroll[1]

[1]School of Science and Technology, Geology Division, University of Camerino, Via Gentile III da Varano, 62032 Camerino, Italy

*email: paola.stabile@unicam.it

Keywords:
Pantellerite glasses, water content, NIR spectroscopy, molar absorptivities.

ABSTRACT

To aid current work on the genesis of pantelleritic magmas, and the desire to use IR spectroscopy to measure water contents in natural (e.g., melt inclusions) and experimental glasses of pantelleritic composition, we have determined molar absorptivities for Near-Infrared (NIR) absorption bands related to molecular water (5200 cm^{-1}) and OH groups (4500 cm^{-1}) in synthetic hydrous pantelleritic glasses, with compositions similar to natural pantellerites from the Eburru complex of the Kenya Rift Valley. The experiments were conducted at P=30 to 150 MPa and T=850-900°C using a synthetic pantelleritic starting composition with (wt%) SiO_2=76.60, Al_2O_3=8.48, FeO*=5.48, K_2O=3.68, Na_2O=4.72 and with molar ratio (Na+K)/Al=1.38. The experiments were H_2O undersaturated (~1.1 to 6.5 wt% H_2O) and the run products were analyzed by Karl-Fischer Titration (KFT) for total dissolved H_2O abundance. Different combinations of baseline types (GG or TT) and intensity measurements (peak height and peak area) were applied to measure both hydroxyl group (OH) and molecular water (H_2O) in the experimental samples. For instance, evaluating the peak heights and using the TT baseline ε_{4500} results to be equal to 0.98(4) (L $mol^{-1}cm^{-1}$) and ε_{5200} to 1.92(2) (L mol^{-1} cm^{-1}); these values differ by ~20 to 50% from published values for metaluminous rhyolitic compositions.

Always consult and cite the final, published document. See http:/www.minsocam.org or GeoscienceWorld

INTRODUCTION

Pantellerites are strongly peralkaline rhyolites characterized by alkali/alumina molar ratios [(Na_2O+K_2O)/Al_2O_3] higher than the unity. Pantellerites are usually richer in Na and Fe and poorer in Al (see trend in MacDonald 1974) than the often associated, less strongly peralkaline comendites (e.g., Scaillet and MacDonald 2003). Both occur in mainly in extensional tectonic settings, from oceanic islands (Ascension Island) to continental rift zones, as for example the Sicily channel rift zone (Pantelleria Island), the Kenyan and Ethiopian Rift Valleys, and Mayor Island (NZ-Taupo Volcanic Zone).

The excess of alkalies over alumina and the higher halogen contents affect the rheological properties of peralkaline magmas, resulting in viscosities that are lower than those of metaluminous silicic magmas. Pantelleritic volcanism can produce large magma volumes and be associated with a variety of eruptive styles, from lava effusion to Plinian activity (Lowenstern and Mahood 1991). Although peralkaline rhyolites were once thought to be relatively H_2O-poor (Bailey and Macdonald 1987), more recent studies indicate magma water contents as high as 5-6 wt% H_2O (e.g., Kovalenko et al. 1988; Webster et al. 1993; Wilding et al. 1993; Barclay et al. 1996), suggesting that melt water contents are relevant to understanding the pantellerite origins, the depth of magma storage and ascent and eruption dynamics.

In fact, overall volatile content, and most importantly water abundance, in rhyolitic magma can influence magma physical properties and crystallization behaviour (e.g. Hammer 2004; Gualda et al. 2012) and in turn rheological properties and

Always consult and cite the final, published document. See http:/www.minsocam.org or GeoscienceWorld

mechanisms, styles and tempo-, of eruptions (Roggensack et al. 1997; Huppert and Woods 2002; Sparks 2003; Cashman 2004; Aiuppa et al. 2007; Edmonds 2008; Stock et al. 2018, Stabile and Carroll, 2020). A large number of studies have been devoted to investigating water abundance in different silicate melt compositions, but only a few experimental studies document water abundances in strongly peralkaline rhyolites and Fe-rich, pantelleritic compositions (e.g. Scaillet and McDonald 2001; Schmidt and Behrens 2008; Di Carlo et al. 2010; Stabile et al. 2018).

To infer quantitative information on volatiles, microanalytical techniques are commonly used on MI trapped in phenocrysts. In particular, near-infrared (NIR) spectroscopy is widely applied to quantify water content in silicate melts and glasses by using the combination bands at 4500 cm^{-1} and 5200 cm^{-1}, respectively assigned to OH groups and molecular H_2O. The absorption peak heights of these bands obey the Lambert-Beer law (e.g. Stolper 1982; Silver et al. 1990) but knowledge of absorption coefficients and density-water content relation are necessary. Both are dependent on the anhydrous glass compositions (Silver et al. 1990; Behrens et al. 1996) but, while the density of the glass can be easily estimated by using experimental determination or empirical calculations, absorption coefficients are known mainly for selected melt compositions (from basalt to rhyolite, see Ohlhorst et al. 2001), and cannot be extrapolated outside of their experimental calibration. Thus, the determination of water content in glass compositions for which the absorption coefficients have not been specifically calibrated may involve large uncertainties. A not-insignificant problem in comparing and extrapolating published data concerning molar absorptivities and glass composition involves the different evaluation methods employed, and in particular the different baseline correction used for measured IR spectra.

Always consult and cite the final, published document. See http:/www.minsocam.org or GeoscienceWorld

For this reason, we have determined IR molar absorption coefficients for both 4500 and 5200 cm^{-1} water bands for hydrous pantelleritic glasses, evaluated by using peak intensity and peak area and employing the two GG- and TT-type (Gaussian and Straight line types, respectively) of baseline correction procedures, commonly used in other published studies of different compositions. The goal of this study is to present new experimental and IR spectroscopic data which can be used to study water contents in MI and glasses of pantelleritic composition. Such studies are, in fact, missing in the literature for these peralkaline compositions, which strongly differ from common calc-alkaline rhyolites used in numerous previous spectroscopic studies (e.g., Newman et al. 1986; Ihinger et al. 1994; Zhang et al. 1997; Withers and Behrens 1999; Ohlorst et al. 2001).

MATERIALS AND METHODS

Experiments were performed using a synthetic peralkaline glass analogue of a pantellerite from the Eburru Volcanic Complex of the Kenyan Rift Valley (Ebu-1 in Scaillet and Macdonald 2006; see also Stabile et al. 2018). The starting material has been prepared from dried oxides and carbonates; the mixture was first ground by hand in an agate mortar and then ground, homogenized and mixed in a disc mill (Siebtechnik Vibratory Disc Mill TS750) for 20 min before melting. The nominal composition of the synthetic pantellerite is, in wt %, SiO_2=76.60, Al_2O_3=8.48, FeO*(total Fe as FeO) =5.48, K_2O=3.68, Na_2O =4.72, with molar (Na+K)/Al=1.38 (Table 1). Glass preparation has been carried out in two steps. At first, the mixture was melted in a platinum crucible using a muffle furnace (Nabertherm P310) at ambient pressure, air atmosphere, and at a temperature of 1600 °C for 2 h and quenched by placing the crucible in a water bath. The resulting glass was crushed and ground and the glass-

Always consult and cite the final, published document. See http:/www.minsocam.org or GeoscienceWorld

powder was melted a second time at 1400 °C for an additional 2 h, before crushing and grinding again in the disc mill to ensure the homogeneity of the glass starting material (see Stabile et al. 2016, 2017 for more details). The powder material (~40 mg per experiment) along with ca. 1–6 wt.% distilled water was loaded into $Ag_{75}Pd_{25}$ capsules (with dimensions of 15 mm length, 3.0 mm inner diameter, 3.4 mm outer diameter). A capsule length of 15 mm was chosen in order to minimize thermal gradient within the capsules and not to exceed the length of the hot zone of the furnaces. The capsules were weighed after each addition of material and then sealed by arc-welding. Weight after welding was checked to verify that water was not lost during welding. For these experiments, we have used water-pressurized cold seal pressure vessels (Nimonic 105) at the Dipartimento di Geologia at University of Camerino (Italy). The oxidation conditions are ~0.8 log $f(O_2)$ units above the Ni-NiO buffer (NNO+0.8), based on previous experiments that used NiO-NiPd $f(O_2)$ sensor capsules (Taylor et al., 1992). Experimental temperatures were from 850 to 900°C, with the higher temperatures used for lower pressure experiments in order to remain above the liquidus: each experiment was run for 168 h (a run duration that, based on previous experience ensures production of samples with homogeneous water distribution). Experimental conditions for each sample are reported in Table 2.

Most of the samples were quenched from experimental conditions to room T by removing the bomb from the furnace and immersing it in a high-pressure stream of compressed air, providing a cooling rate of ~120 °C/min. Rapid-quench bombs have been used for several experiments in order to verify - given the same T, P conditions - whether the cooling rate influenced the absorption coefficients values (Behrens et al. 1996; Zhang et al. 1997; Withers and Behrens 1999). For these samples, quenching occurred within a few seconds by dropping the sample capsule from the hot top part of

Always consult and cite the final, published document. See http:/www.minsocam.org or GeoscienceWorld

the vessel into the cooled part of the pressure seal by lowering a cylindrical magnet supporting the sample assembly to the base of the stainless-steel extension (e.g., as described in Carroll and Blank, 1997). During all high-pressure experiments, the quench was isobaric because constant pressure was maintained during cooling by using a large-volume pressure reservoir and a hand-operated pressure generator.

After the quench, capsules were again weighed to check for leaks and opened. All samples were quenched rapidly enough to produce homogenous, crystal-free glasses. The absence of crystallinity has been verified by means of optical microscope and X-ray Powder diffraction (XRD) (see Supplementary Data 1). All the glasses were also analysed by electron microprobe (EMP) before being used for Karl-Fisher Titration (KFT) and Fourier Transform Infrared Spectroscopy (FTIR) analyses.

Electron Microprobe

The chemical composition of each experimental glass was analyzed by EMP using a CAMECA SX50 at the Consiglio Nazionale delle Ricerche (CNR)–Institute of Geosciences and Earth Resources (IGG)- in Padova. The measurements were performed with an acceleration voltage of 20 KeV, a defocused beam of 8μm and a beam current of 20nA for Fe, Ca and Mg, while a beam current of 2 nA has been used for K, Na, Al and Si (measured first). Each sample was measured on 5 to 10 random locations to check for homogeneity and within error all samples were homogeneous. Individual oxide values, normalized to 100% total, and the starting glass composition, are reported in Table 1 and values are comparable with only some slight variations for Na and K (well-known for difficulty to analyze by electron microprobe in hydrous glasses).

Always consult and cite the final, published document. See http:/www.minsocam.org or GeoscienceWorld

Karl-Fisher Titration

The KFT analyses for determination of total water content in experimental samples were done at the Institute of Mineralogy of the University of Hannover. In this procedure, H_2O is extracted by placing 10-20 mg of sample into a Pt crucible in an induction furnace and heating the sample up to 1300°C. In the presence of specific reagents, water reacts quantitatively with colorimetrically generated iodine and the liberated H_2O is then transported by a dry Ar stream to the titration cell. The maximum uncertainty of the titration rate for a sample mass of 10 mg is usually of ca. 0.15 H_2O wt% (Holtz et al. 1995; Behrens 1995). A detailed description of the KFT method is given in Behrens et al. (1996). A critical aspect to be considered when employing dehydration techniques is whether or not all the water has been released from the sample. Subsequent FTIR measurements of the glasses allow establishing if all the water in the glasses has been extracted by KFT. It has been already reported in literature studies that the extraction of water results to be incomplete in silicic melts containing initially more than 1.5 wt.% H_2O (Behrens 1995; Ohlhorst et al. 2001; Leschik et al. 2004). For this reason, water contents determined by KFT have all been corrected by adding 0.10 wt% to account for unextracted water (Table 2).

Density determination

Densities of anhydrous pantelleritic glasses were measured by weighing the single glass pieces in air and in water. For glass pieces of size >200 mg the uncertainty in density determination was < 1%. The obtained density data were used to calculate the density of hydrous glasses using the procedure proposed by Lange and Carmichael (1987). According to this, the molar volume of natural silicate melts can be described as a linear function of composition, temperature, pressure and volatile components (as included

Always consult and cite the final, published document. See http:/www.minsocam.org or GeoscienceWorld

This is a preprint, the final version is subject to change, of the American Mineralogist (MSA)
Cite as Authors (Year) Title. American Mineralogist, in press.
DOI: https://doi.org/10.2138/am-2020-7363

by model equations). Uncertainties in calculated densities of hydrous glass samples are estimated to be 5 g/L.

FTIR Spectroscopy

Doubly polished glass chips of experimental samples were cleaned ultrasonically in acetone and ethanol and examined under petrographic microscope before FTIR measurements in the laboratory of Dr. Bjorn Mysen, Geophysical Laboratory, Carnegie Institution for Science, Washington D.C., USA. Spectra were recorded in the near–infrared (NIR) using a halogen light source, a CaF_2 beamsplitter and an InSb detector. The scan range was 7800–750 cm^{-1} at a 4-8 cm^{-1} resolution and 1024-4096 accumulations. Absorption spectra of the glass slabs with thickness ranging from ~50 to ~500 μm (measured with Mitutoyo digital micrometer; precision ±1 μm) were recorded using a Jasco model IMV4000 FTIR microscope system operating in transmission mode with 10X objective and condenser Cassegrainian lens. Each sample chip was placed on 2 mm thick IR transparent BaF_2 window and measured at different spots (3-5 spectra per sample) using a 100x100 μm slit aperture.

NIR RESULTS

Water content obtained by KFT, thickness and density of the samples, absorbance and integrated intensity are all reported in Table 2.

Analyses of IR spectra

For the determination of molecular H_2O and OH concentrations, the two bands at 5200 and 4500 cm^{-1} are the most useful for typical geological samples. We did not consider the first overtone near 7100 cm^{-1} because it is usually too weak, except for very thick

Always consult and cite the final, published document. See http:/www.minsocam.org or GeoscienceWorld

samples or those with high total water. On the other hand, the 3550 cm^{-1} band, often used to estimate water in minerals (i.e. at low water content), was not used because H_2O abundances in our experiments would have required extremely thin sample in order to not have overwhelmingly strong absorbance values.

In the higher wavenumber range (> 5700 cm^{-1}) some collected spectra displayed a rising background, most likely related to crystal field transition of divalent iron (e.g. Ohlhorst et al. 2001; Mandeville et al. 2002), but we did not treat or make any interpretation of these spectral features during this work and they do not affect our determination of backgrounds of water-related absorbance peaks, as discussed below.

Near infrared spectra of three glasses with different total water content are shown in Figure 1 and arranged in order of increasing total water content from bottom to the top. Two clear water-related bands near 4500 and 5200 cm^{-1} are visible in all spectra. The band at 4500 cm^{-1} is assigned to the combination of stretching and bending of OH group and the band at 5200 cm^{-1} to the combination of stretching and bending mode of H_2O molecules (e.g. Scholze 1960; Bartholomew et al. 1980; Stolper 1982). Exact position of the hydroxyl groups and molecular water bands varies from 4506 to 4492 cm^{-1} and 5236 to 5233 cm^{-1}, respectively, with increasing total water content.

In addition, a broader small band near 4000 cm^{-1} is also visible in all the spectra and it appears well separated from the 4500 cm^{-1} peak. However, this peak is positioned at the flank of the OH absorption at ca. 3600 cm^{-1} (Davis and Tomozawa 1996; Withers and Behrens 1999; Efimov and Pogareva 2006) and it makes difficult to extract quantitative information from the 4000 cm^{-1} peak. For this reason, the 4000 cm^{-1} peak has not been used for the determination of glass water contents, although it may involve

Always consult and cite the final, published document. See http:/www.minsocam.org or GeoscienceWorld

different combination modes of both OH and H_2O species that are not identified (Le Losq et al. 2015 and references therein).

Baseline Correction Procedures

To measure the intensity of an absorption band and determine the total water and water speciation, an appropriate baseline must be subtracted under the peaks near 4500 and 5200 cm^{-1}. The choice of the baseline correction procedure can affect the intensity and thus the calculated species concentrations. For this reason, and following previous studies (e.g. Withers and Behrens 1999; Ohlhorst et al. 2001; Mandeville et al. 2002), we have tested two types of baselines: simple straight lines under the 4500 and 5200 cm^{-1} bands (also called TT baseline), and a combination of a Gaussian curve and a straight line (or GG baseline). We did not consider the flexicurve or French curve (FC) technique because it resulted to be an extremely subjective procedure (e.g. Newman et al. 1986; Zhang et al. 1997).

At first attempt we used tangents under both bands at ca. 4500 and 5200 cm^{-1}, i.e. we employed the so-called TT baseline type procedure (Figure 2). This is the simplest procedure for baseline correction and easily reproducible, but it could be sometimes a rough approximation leading to underestimate the area of the OH band or, furthermore, to return lower intensities due to the presence of the nearby ~4000 cm^{-1} band (see e.g. Withers and Behrens 1999).

For the above reasons, we have decided to adopt also the GG baseline approach where a baseline and a Gaussian are both subtracted from the NIR spectrum. Thus, following Withers and Behrens (1999), we have fitted a linear baseline to the 5200 cm^{-1} peak

Always consult and cite the final, published document. See http:/www.minsocam.org or GeoscienceWorld

region and one gaussian to the 4000 cm^{-1} peak. Using the GG approach allowed us to satisfactorily model, in highly reproducible way, the background in the wavenumber range of interest (Figure 2). This procedure is slightly different from the GG baseline approach used by Ohlhorst et al. (2001), who used two Gaussian curves, one near the 4000 cm^{-1} peak and the second one at the iron-related band near 5700 cm^{-1}. The latter one was, instead, not necessary to fit the background at the high-frequency range (above 5200 cm^{-1}) of our compositions or of the iron-poor rhyolitic compositions studied by Withers and Behrens (1999).

Different approaches for the baseline correction can produce different results because samples of a specific composition show spectral variations in terms of the background, in either the low frequency range (<4200 cm^{-1}) or the higher one (above 5200 cm^{-1}). Thus, to avoid such problem and make any baseline correction procedure both precise and reproducible, sufficiently detailed information about the fitting approach used should always be provided.

Calibration of molar absorption coefficients

The concentrations of molecular and hydroxyl water were calculated from peak heights and peak areas using the Lambert-Beer law:

$$C_{H2O}=\frac{1802 A_{H2O}}{d\rho}\cdot\frac{1}{\varepsilon_{H2O}} \quad [1]$$

$$C_{OH}=\frac{1802 A_{OH}}{d\rho}\cdot\frac{1}{\varepsilon_{OH}} \quad [2]$$

Where A is the absorbance (peak height), d is the thickness in cm and ρ the density in g/l, ε the linear molar absorption coefficient in l mol^{-1} cm^{-1}, C_{OH} and C_{H2O} are the

Always consult and cite the final, published document. See http:/www.minsocam.org or GeoscienceWorld

This is a preprint, the final version is subject to change, of the American Mineralogist (MSA)
Cite as Authors (Year) Title. American Mineralogist, in press.
DOI: https://doi.org/10.2138/am-2020-7363

concentrations of hydroxyl group and molecular water, respectively, in wt %. When no other water species are present besides H_2O and OH, the concentration of total water (C_{water}) can be given as:

$$C_{water} = C_{H2O} + C_{OH} \quad [3]$$

Thus, if we combine the Equations 1 and 2 we obtain the following relation:

$$\left[\frac{1802 A_{H2O}}{d\rho c_{water}}\right] = \varepsilon_{H2O} - \left[\frac{\varepsilon_{H2O}}{\varepsilon_{OH}} \cdot \frac{1802 A_{OH}}{d\rho c_{water}}\right] \quad [4]$$

This equation can be directly used for the determination of the molar absorption coefficients and by plotting the normalized absorbances against each other, a linear regression of data over a range of water contents will produce a plot (see Fig. 3) where the intercepts on the Y-and X-axes directly provide the values of ε_{H2O} and ε_{OH}.

When we use peak areas instead of peak heights, A will be replaced by A* (integrated intensity in cm^{-1}) and by ε* (integral molar absorption coefficient in $l\ mol^{-1}cm^{-2}$). Normalized absorbances and normalized intensities combined for both TT- and GG-type of baseline are plotted in Figures 3 and reported in Table 2. The scatter of the data is slightly larger when considering peak areas (Figure 3b), most likely as a consequence of the greater sensitivity of peak areas to the choice of background.

Errors in water content calculated, along with molecular H_2O and OH abundances, are defined taking into account all the different uncertainties in the variables present in Equation 1 (absorbance, sample thickness and glass density).

Always consult and cite the final, published document. See http:/www.minsocam.org or GeoscienceWorld

DISCUSSION AND CONCLUSIONS

Evaluating the peak heights and using the TT type baseline, ε_{4500} is 0.98(4) (L mol^{-1} cm^{-1}) and ε_{5200} is 1.92(2) (L mol^{-1}cm^{-1}), whereas using the GG baseline, ε_{4500} is 1.00(4) (L mol^{-1}cm^{-1}) and ε_{5200} is 2.01(2) (L mol^{-1} cm^{-1}). Small deviations result from the evaluation of peak areas by using the two types of baseline, but values are approximately equal within the errors, with ε^*_{4500} = 218(20) (L mol^{-1}cm^{-2}) and ε^*_{5200} 245(23) (L mol^{-1}cm^{-2}) using the TT type baseline, and ε^*_{4500} = 229(40) (L mol^{-1}cm^{-2}) and ε^*_{5200} 295(39) (L mol^{-1}cm^{-2}) using the GG baseline.

The ε values, which have been defined by the intercepts of the least-squares fits to the lines in Figure 3a-b, were determined assuming that the intensities of the bands are linearly related to species concentrations, as done in previous works (e.g. Stolper 1982; Newman et al. 1986; Silver et al. 1990; Behrens et al. 1999; Ohlhorst et al. 2001). However, the assumption of constant molar absorptivities in glasses has not been always observed to hold. For instance, Zhang et al. (1997) found that at total water content > 2.7 wt% in rhyolitic glass, the linear relation between peak intensity and species concentrations did not apply, and they proposed a total water content dependence of molar absorption coefficients to explain the results they obtained.

Perhaps more importantly, other studies have shown a dependence of molar absorptivities on melt composition, including silica content, Na/K ratio, or excess of alkali to aluminium (Stolper 1982; Silver et al. 1990; Behrens et al. 1996). We made an attempt to investigate the possible effect of silica content, Na/K and peralkalinity (expressed as [(Na + K)/Al] molar ratio) on the ε values obtained, but we found no clear, simple correlation between ε and these melt composition parameters.

Always consult and cite the final, published document. See http:/www.minsocam.org or GeoscienceWorld

DOI: https://doi.org/10.2138/am-2020-7363

Ohlhorst et al. (2001) found a systematic increase of ε from basaltic to andesitic to rhyolitic compositions and they used SiO_2 as a proxy to describe the compositional dependence of the absorption coefficients in the 3 compositions they studied. They observed that a simple parabolic equation could be appropriate to predict ε for glasses of intermediate melt compositions, stating that interpolation or extrapolation would have been very uncertain. We used the same equation for our pantelleritic melts- since pantellerites are peralkaline rhyolites with intermediate silica content between basalt and rhyolite- but it produced calculated H_2O contents significantly less (and OH values higher) than our measured values (for example ε_{OH} and ε_{H2O} TT obtained by using Ohlhorst and co-authors equation were equal to 1.4 and 1.6 L $mol^{-1}cm^{-1}$, respectively), suggesting that we may need to account for the effect of other compositional parameters, especially in complex multicomponent systems. Previously, also Dixon et al. (1995) tried to correlate the two water absorption bands for basaltic and other silicate melt compositions with the cation fraction of tetrahedral cations (τ), where τ was determined as the ratio between the sum of (Si^{4+} +Al^{3+})/total cations. Dixon and co-authors found that both ε_{4500} and ε_{5200} determined in several laboratories on different glass compositions correlate positively and linearly with the sum of the cation fractions of Si and Al. This suggests that, although other compositional variables clearly influence the values of molar absorptivities, such linear relationships can be used to predict the molar absorptivities of hydrous species in glasses to within ± 20% when they have not been measured directly, as also reported by Mandeville et al. (2002). Similarly, we calculated the cation fraction of tetrahedral cations (τ) in our pantelleritic compositions and for different silicate melts (Table 3), to look for systematic variations in molar absorptivities. It appears that pantellerites are most similar to rhyolitic compositions studied by Wither and Behrens (1999) in terms of mole fraction of

Always consult and cite the final, published document. See http:/www.minsocam.org or GeoscienceWorld

network-forming cations (τ, in Table 3), although molar absorptivity values differ significantly, as discussed below.

These observations support the idea that direct calibrations for the compositions of interest will yield the most accurate quantitative results, as clearly stated also by Dixon et al. (1995) and later by Mandeville et al. (2002), and there are not fully satisfactory models that can be used as valid alternative to the considerable work of calibration, thus clearly satisfying the scope of this work.

Water speciation

The proportions of H_2O species present as molecular water and hydroxyl groups in pantelleritic glasses are reported as a function of total H_2O content in Figures 4a-b. Figure 4a reports the data fitted by using the absorbances in both the baseline procedures TT and GG, while Figure 4b refers to data gained by dealing with integrated intensities of the NIR spectra. Samples with total H_2O content less than roughly 3.5 wt% have OH^- as the dominant water species, but when the total H_2O increases the same samples show an increasing content of molecular H_2O and nearly constant OH^- concentrations (see both Figures 4a-b). These findings are consistent with previous studies on hydrous silica-rich glasses (e.g. Stolper et al. 1982; Newman et al. 1986; Carroll and Blank 1997; Withers and Behrens 1999).

Both combinations of baseline-fitting procedures reproduce the same water dissolution mechanisms, where OH species is more abundant at low H_2O_{tot} while molecular H_2O becomes dominant for higher total H_2O contents (above ~3-4 wt% H_2O). The water values related to molecular water, hydroxyl group and total water content of all the

Always consult and cite the final, published document. See http:/www.minsocam.org or GeoscienceWorld

samples along with relative errors calculated considering combined uncertainties of different variables of Equation (1) are reported in Table 1 and 2 in Supplementary Data 2.

Using the GG/ and TT/ peak height procedure, the differences between the two water species concentrations (c_{H2O} and c_{OH}) are, in fact, almost identical within errors (maximum-minimum values of 4.6(0.5)-0.3(0.03) and 2.2(0.2)-0.7(0.1) for TT-type baseline approach, and 4.3(0.4)-0.3(0.03) and 2.3(0.3)-0.7(0.1) for GG-type baseline). When using the peak area of the FTIR spectra, we can discern only slight differences for the water species values obtained by the two different TT- and GG-type baseline approaches. In particular, in this latter case, maximum and minimum values of c_{H2O} and c_{OH} obtained by the peak area procedure are 5.2(0.5)-0.36(0.04) and 1.8(0.2)-0.6(0.1) when the TT-type baseline is used, while water results in terms of c_{H2O} and c_{OH} are 4.7(0.5)-0.3(0.03) and 2.3(0.2)-0.70(0.1) when the GG-type baseline is used.

Consequently, we can state that at given total water content of the glass the relative amount of H_2O and OH is almost equal within the errors if determined by using the peak height/area and GG/TT baseline procedure, with the only exception being a slightly higher value of molecular H_2O when using the TT baseline fitting which accounts for the peak area of the 5200 cm^{-1} band.

The relative proportions of molecular H_2O and hydroxyl species present in the quenched samples do not reflect the speciation in the melt at the elevated temperatures and pressures of the experiments (e.g., Zhang et al., 1995), but without knowledge of how speciation varies with quench rate, or in situ measurements, it is not possible to be more quantitative about speciation in high temperature melts (Silver et al. 1990; Dingwell and Webb 1990; Keppler and Bagdassarov, 1993; McMillan

Always consult and cite the final, published document. See http:/www.minsocam.org or GeoscienceWorld

1994; Zhang et al. 1995; Nowak and Behrens 1995; Carroll and Blank, 1997). However, it is quite clear that the abundances of hydroxyl and molecular water may be influenced by significant reequilibration during quenching, and these quenching effects lead to an increased abundance of molecular H_2O in comparison with the amount originally present in the melt at high temperature (Stolper 1989; Silver et al. 1990; Zhang et al. 1995; Nowak and Behrens 1995). Based on our 2 samples subjected to rapid quenching (<1 min) compared with the more abundant air-quenched samples (~6-7 min), we observed no variation of the resulting total water content and/or water species ratios with quenching rate of the melt. If we consider the final concentrations of OH and H_2O result from the continuous reaction and re-equilibration during the cooling history of the sample, we can observe similar OH/H_2O ratios of 1.1 and 1.2 for c_{water} of 3.2(0.5) and 3.0(0.4), respectively for fast quench (FQ) and slow quench (SQ) experiments. This can give information about the apparent equilibrium temperature T_{ae} (Zhang, 1994; Zhang et al. 1999), which is the hypothetical equilibrium temperature corresponding to the final speciation and it is usually low for small OH/H_2O ratios and slow cooling rates. Here, the similar OH/H_2O ratios indicate that the two different quench rates investigated lead to the same T_{ae} at a given c_{water} in our glasses. Furthermore, spectroscopic data related to the two rapidly quenched samples fit well to the same calibration curves defined by the other glass samples produced in slow quench experiments. Thus, this means that no noticeable influence of cooling rate on the molar absorption coefficients can be observed in our samples.

Similarly, Withers and Behrens (1999) have investigated the possible effect of quenching on rhyolitic glasses containing around 3 and 5 wt.% H_2O. Glasses with initial OH/H_2O ratios of 1.00 and 0.60 were reheated at 800 °C and at 300 MPa and quenched

Always consult and cite the final, published document. See http:/www.minsocam.org or GeoscienceWorld

This is a preprint, the final version is subject to change, of the American Mineralogist (MSA)
Cite as Authors (Year) Title. American Mineralogist, in press.
DOI: https://doi.org/10.2138/am-2020-7363

rapidly, resulting in an increase in OH/H_2O ratios to 1.17 and 0.72, respectively. From their results, accounting also for the good fitting of the different sets of data (obtained by slow and fast quench experiments) on the same calibration curve, they inferred that no clear effect of quenching rate was evident (at least at high water content). On the other hand, Zhang et al. (1997) have shown that at low total water contents, not only the species concentrations but also the apparent total water contents are dependent on cooling rate when constant molar absorption coefficients are used. However, given the number of samples we have produced, and the range of total water content investigated (1.09 to 6.53 wt% H_2O_{total}), at present we cannot quantify how molar absorption coefficients might depend on sample thermal history or total H_2O.

Comparison with previous data

Molar absorption coefficients for OH and H_2O combination bands for different hydrous melt compositions from the literature are reported in Table 3 along with our values. The absorption coefficients for our pantelleritic melts differ from those of similar silica-rich compositions, such as the metaluminous rhyolites studied by Withers and Behrens (1999). In fact, the absorption values for OH for pantellerite (GG and TT, peak heights) are much lower than the metaluminous rhyolite values reported by Withers and Behrens (1999), while the absorption coefficients for H_2O are slightly higher. On the other hand, our absorptivities for OH are similar to dacite values reported by Ohlhorst et al. (2001), but our molar absorptivities for molecular H_2O are significantly higher.

These observations indicate that using molar absorptivities derived from metaluminous rhyolitic compositions are not appropriate for peralkaline pantelleritic melts/glasses and

Always consult and cite the final, published document. See http:/www.minsocam.org or GeoscienceWorld

would likely underestimate hydroxyl water and overestimate molecular water in pantelleritic melt compositions like the ones here investigated.

The observed variations in molar absorptivities in published studies can be linked to several causes of different nature. These include the following: -interlaboratory differences in analytical equipment- including IR beam splitters, detectors, IR sources- that can produce up to 10% differences in measured peak heights for water bands for the same glass even when the same linear background subtraction used (see Behrens et al. 1996); -the different method of background correction or baseline fitting (see Ohlhorst et al. 2001, or this study for review); - Fe-free glasses present higher τ and higher molar absorptivities for both 4500 and 5200 cm^{-1} peaks compared with Fe-bearing glasses (see for example Fe-free and Fe-bearing andesite of Mandeville et al. 2002). Considering the large number of factors and variables that can affect the determination of molar absorptivity of water bands for a specific silicate melt composition, at present it appears that the most accurate way is, when possible, a direct calibration for the composition of interest.

Overall, our results indicate that use of constant-valued molar absorptivities can reproduce the KFT-measured H_2O contents up to at least 6.53 wt% total H_2O, as shown in Figure 5. The fit quality is very good up to ~ 4 wt% total H_2O, independent of the background fitting procedure adopted. For water contents higher than 4 wt%, the data slightly scatter from the ideal correlation line, possibly resulting from the different water speciation mechanisms at higher total water contents, but differences are within the relative errors. Because the KFT data were used to obtain best-fit molar absorptivities, the correlation in Figure 5 is most useful to demonstrate that constant-valued molar absorptivites are a good approximation for pantelleritic glasses up to the maximum total H_2O content investigated (6.53 wt%).

Always consult and cite the final, published document. See http:/www.minsocam.org or GeoscienceWorld

IMPLICATIONS

The results of this study provide new values of molar absorptivities, useful for measurement of water contents in natural pantelleritic glasses and melt inclusions. In addition, we have shown that it is not appropriate to use molar absorptivities determined for metaluminous rhyolites for determining water contents of pantelleritic glasses as this will lead to large underestimation of total H_2O contents, especially for total H_2O contents less than 4-5 wt% (based on large differences in molar absorptivity for hydroxyl water in pantellerite and metaluminous rhyolite, shown in Table 3). As previous studies (e.g., Lowenstern and Mahood 1991; Barclay et al. 1996) have noted, pantelleritic magmas can show a wide diversity in eruptive styles, from lava flows, to strombolian fire fountains, to Plinian explosive eruptions. Understanding and/or modelling the dynamics of such variable eruption styles requires accurate data for magma water contents and our new molar absorptivity data will facilitate accurately characterizing melt water contents in pantelleritic systems.

ACKNOWLEDGEMENTS

The authors thank R. Carampin (Electron Microprobe Laboratory of CNR- Institute of Geosciences and Earth Resources (IGG)- Padova) for microprobe analyses, H. Behrens and the KFT laboratory of the Institute of Mineralogy (University of Hannover, Germany) for water determination, and B. Mysen and the Geophysical Laboratory of the Carnegie (Institution for Science, Washington D.C., USA) for assistance with Infrared Spectroscopy measurements. We are grateful to Charles Le Losq and Jake Lowenstern for their valuable comments during the revision of the manuscript. The

Always consult and cite the final, published document. See http:/www.minsocam.org or GeoscienceWorld

authors also thank Sara Fanara and Francesco Radica for useful discussion. This research has been supported by the LIFE Project to E.P. (LIFE14 ENV/IT/000801 ECO TILES), FAR 2012 and PRIN2017 to M.R.C, and FIRB (grant n. RBFR082WRU) to G.G.

REFERENCES

Aiuppa, A., Franco, A., Von Glasow, R., Allen, A.G., D'Alessandro W., Mather, T.A., Pyle, D.M., and Valenza, M. (2007) The tropospheric processing of acidic gases and hydrogen sulphide in volcanic gas plumes as inferred from field and model investigations. Atmospheric Chemistry and Physics, 7, 1441–1450.

Bailey, D. K. and Macdonald, R. (1987). Dry peralkaline felsic liquids and carbon dioxide flux through the Kenya rift zone. In: Mysen, B. (ed.) Magmatic Processes: Physicochemical Principles. Geochemical Society, Special Publication 1, 91-105.

Barclay, J., Carroll, M. R., Houghton, B. F., and Wilson, C. J. N. (1996). Preeruptive volatile content and degassing history of an evolving peralkaline volcano. Journal of Volcanology and Geothermal Research 74, 75-87.

Bartholomew, R.F., Butler, B.L., Hoover, H.L., and Wu, C.K. (1980) Infrared spectra of a water-containing glass. American Ceramic Society Journal, 63, 481–485.

Always consult and cite the final, published document. See http:/www.minsocam.org or GeoscienceWorld

This is a preprint, the final version is subject to change, of the American Mineralogist (MSA)
Cite as Authors (Year) Title. American Mineralogist, in press.
DOI: https://doi.org/10.2138/am-2020-7363

Behrens, H., Romano, C., Nowak, M., Holtz, F., and Dingwell, D.B. (1996) Near-infrared spectroscopic determination of water species in glasses of the system MAlSi3O8 (M=Li, Na, K): an interlaboratory study. Chemical Geology, 128, 41–63.

Behrens H. (1995) Determination of water solubilities in high-viscosity melts: an experimental study on NaAlSi3O8. European Journal of Mineralogy, **7**, 905-920.

Carroll, M.R., and Blank, J.G. (1997) The solubility of H2O in phonolitic melts. American Mineralogist, 82, 1111 –1115.

Cashman, K. V. (2004) Volatile controls on magma ascent and eruption. In: Sparks, R. S. J. & Hawkesworth, C. J. (eds.) The State of the Planet: Frontiers and Challenges in Geophysics. American Geophysical Union, 109-124.

Davis, K.M. and Tomozawa, M. (1996) An infrared spectroscopic study of water-related species in silica glasses. Journal of Non-Crystalline Solids, 201, 177–198.

Di Carlo, I., Rotolo, S., Scaillet, B., Buccheri, V., and Pichavant, M. (2010) Phase Equilibrium Constraints on Pre-eruptive Conditions of Recent Felsic Explosive Volcanism at Pantelleria Island, Italy. Journal of Petrology, 51 (11), 2245-2276.

Dingwell, D.B., and Webb, S.L. (1990) Relaxation in silicate melts. European Journal of Mineralogy, 2, 427–449.

Dixon, T.E., Stolper, E., and Holloway, J.R. (1995) An experimental study of water and carbon dioxide solubilities in mid-ocean basalt liquids: Part I. Calibration and solubility models. Journal of Petrology, 36, 1607–1631.

Always consult and cite the final, published document. See http:/www.minsocam.org or GeoscienceWorld

This is a preprint, the final version is subject to change, of the American Mineralogist (MSA)
Cite as Authors (Year) Title. American Mineralogist, in press.
DOI: https://doi.org/10.2138/am-2020-7363

Edmonds, M., McGee, K.A., and Doukas, M.P. (2008) Chlorine degassing during the lava dome-building eruption of Mount St. Helens, 2004–2005, chapter 27 *of* Sherrod, D.R., Scott, W.E., and Stauffer, P.H., eds., A volcano rekindled; the renewed eruption of Mount St. Helens, 2004–2006. *U.S.* Geological Survey Professional Paper, 1750, 573-589.

Efimov, A.M. and Pogareva, V.G. (2006) IR absorption spectra of vitreous silica and silicate glasses: The nature of bands in the 1300 to 5000 cm−1 region. Chemical Geology, 229, 198–217.

Gualda, G.A.R., Ghiorso, M.S., Lemons, R.V., and Carley, T.L. (2012) Rhyolite-MELTS: a modified calibration of MELTS optimized for silica-rich, fluid-bearing magmatic systems. Journal of Petrology, 53, 875–890.

Hammer, J.E. (2004) Crystal nucleation in hydrous rhyolite: Experimental data applied to classical theory. American Mineralogist, 89, 1673–1679.

Holtz, F., Behrens, H., Dingwell, D.B., and Wilhelm, J. (1995) H_2O solubility in haplogranitic melts: compositional, pressure and temperature dependence. American Mineralogist, 80, 94– 108.

Huppert, H. E., and Woods, A. W. (2002) The role of volatiles in magma chamber dynamics. Nature, 420, 493-495.

Ihinger, P.D., Hervig, R.L., and McMillan, P.F. (1994) Analytical Methods for Volatiles in Glasses, In Carroll, M.R., and Holloway, J.R., Eds., Volatiles in Magmas, 30, 67–121. Reviews in Mineralogy, Mineralogical Society of America, Washington, D.C.

Always consult and cite the final, published document. See http:/www.minsocam.org or GeoscienceWorld

This is a preprint, the final version is subject to change, of the American Mineralogist (MSA)
Cite as Authors (Year) Title. American Mineralogist, in press.
DOI: https://doi.org/10.2138/am-2020-7363

Keppler, H., and Bagdassarov, N. S. (1993). High-temperature FTIR spectra of H_2O in rhyolite melt to 1300°C. Am. Mineral. 78, 1324-1327.

Kovalenko, V.I., Herving, R.L., and Sheridan, M.F., (1988) Ion-microprobe analyses of trace elements in anorthoclase, hedembergite, aenigmatite, quartz, apatite and glass in Pantellerite: evidence for high water content in pantellerite melt. Am. Mineral. 73, 1038–1045.

Lange, R.A., and Carmichael, I.S.E. (1987) Densities of Na2O-K2O-CaO- MgO-FeO-Fe2O3-Al2O3-TiO2-SiO2 liquids: new measurements and derived partial molar properties. Geochimica et Cosmochimica Acta, 51, 2931-2946.

Le Losq, C., Cody, G. D., and Mysen, B. O. (2015). Complex IR spectra of OH- groups in silicate glasses: Implications for the use of the 4500 cm^{-1} IR peak as a marker of OH- groups concentration. American Mineralogist, 100(4), 945–950.

Leschik, M., Heide, G., Frischat, G.H., Behrens, H., Wiedenbeck, M., Wagner, N., Heide, K., Geißler, H., and Reinholz, U. (2004) Determination of H2O and D2O contents in rhyolitic glasses. Physic and Chemistry of Glasses, 45, 238–251.

Lowenstern, J.B., and Mahood, G.A. (1991) New data on magmatic H_2O contents of pantellerites with implications for petrogenensis and eruptive dynamics at Pantelleria. Bull Volcanol 54, 78-83.

Macdonald, R. (1974). Nomenclature and petrochemistry of the per- alkaline oversaturated extrusive rocks. Bulletin of Volcanology 38, 498-505.

Mandeville, C.W., Webster, J.D., Rutherford, M.J., Taylor, B.E., Timbal, A., and Faure, K. (2002) Determination of molar absorptivities for infrared absorption bands of H2O in andesitic glasses. American Mineralogist, 87, 813–821.

Always consult and cite the final, published document. See http:/www.minsocam.org or GeoscienceWorld

This is a preprint, the final version is subject to change, of the American Mineralogist (MSA)
Cite as Authors (Year) Title. American Mineralogist, in press.
DOI: https://doi.org/10.2138/am-2020-7363

McMillan, P. F. (1994) Water solubility and speciation models. Review in Mineralogy, 30, 131- 156.

Newman, S., Epstein, S., and Stolper, E. (1986) Measurement of water in rhyolitic glasses: Calibration of an infrared spectroscopic technique. American Mineralogist, 71,1527–1541.

Nowak, M., and Behrens, H. (1995) The speciation of water in haplogranitic glasses and melts determined by in situ near-infrared spectroscopy. Geochimica et Cosmochimica Acta. 59, 504–511.

Ohlhorst, S. Behrens, H., and Holtz, F. (2001) Compositional dependence of molar absorptivities of near infrared OH– and H2O bands in rhyolitic to basaltic glasses. Chemical Geology, 174, 5–20.

Roggensack, K., Hervig, R. L., McKnight, S. B., and Williams, S. N. (1997) Explosive basaltic volcanism from Cerro Negro volcano: influence of volatiles on eruptive style. Science 277, 1639-1642.

Scaillet, B., and MacDonald, R. (2006) Experimental and thermodynamic constraints on the sulphur yield of peralkaline and metaluminous silicic flood eruptions. Journal of Petrology, 47, 1413-1437.

Scaillet, B. and Macdonald, R. (2003). Experimental constraints on the relationships between peralkaline rhyolites of the Kenya Rift Valley. Journal of Petrology 94, 1867-1894.

Scaillet, B., and Macdonald, R. (2001). Phase relations of peralkaline silicic magmas and petrogenetic implications. Journal of Petrology, 42, 825-845.

Always consult and cite the final, published document. See http:/www.minsocam.org or GeoscienceWorld

Schmidt, B., and Behrens, H. (2008) Water solubility in phonolite melts: Influence of melt composition and temperature. Chemical Geology, 256, 259–268.

Scholze, H. (1960) Zur Frage der Unterscheidung zwischen H2OMolekeln und OH-Gruppen in Gla¨sern und Mineralen. Naturwissenschaften, 47, 226–227.

Silver, L.A., Ihinger, P.D., and Stolper, E. (1990). The influence of bulk composition on the speciation of water in silicate glasses. Contribution to Mineralogy and Petrology, 104, 142–162.

Sparks, S. R. J. (2003) Dynamics of magma degassing. Geological Society of London, Spec. Publ. 213, 5–22.

Stock, M. J., Humphreys, M. C. S., Smith, V. C., Isaia, R., Brooker R.A., and Pyle, D. M. (2018) Tracking volatile behaviour in sub-volcanic plumbing systems using apatite and glass: insights into pre-eruptive processes at Campi Flegrei, Italy. Journal of Petrology, 59(12), 2463-2492.

Stabile, P., Webb, S., Knipping, J.K, Behrens, H., Paris, E., and Giuli, G. (2016) Viscosity of pantelleritic and alkali-silicate melts: Effect of Fe redox state and Na/(Na+K) ratio. Chemical Geology, 422,73-82.

Stabile, P., Giuli, G., Cicconi, M.R., Paris, E., Trapananti, A., and Behrens, H. (2017) The effect of oxygen fugacity and Na/(Na+K) ratio on iron speciation in pantelleritic glasses. Journal of Non-Crystalline Solids, 478.

Always consult and cite the final, published document. See http:/www.minsocam.org or GeoscienceWorld

Stabile, P., Radica, F., Bello, M., Behrens, H., Carroll, M.R., Paris, E., and Giuli, G. (2018) H_2O solubility in pantelleritic melts: Pressure and alkali effects. Neues Jahrbuch für Mineralogie - Abhandlungen (J-Min-Geochem), 195(1).

Stabile, P., and Carroll, M. R. (2020) Petrologic experimental data on Vesuvius and Campi Flegrei magmatism: a review, Editor(s): Benedetto De Vivo, Harvey E. Belkin, Giuseppe Rolandi, Vesuvius, Campi Flegrei, and Campanian Volcanism, Elsevier, 323-369.

Stolper, E. (1982) Water in silicate glasses: an infrared spectroscopic study. Contributions to Mineralogy and Petrology, 81, 1–17.

Taylor, J. R., Wall, V. J., and Pownceby, M. I. (1992) The calibration and application of accurate redox sensors. American Mienralogist, 77, 284–295.

Webster, J. D., Taylor, R. P. and Bean, C. (1993) Pre-eruptive melt com- position and constraints on degassing of a water-rich pantellerite magma, Fantale volcano, Ethiopia. Contributions to Mineralogy and Petrolog 114, 53-62.

Wilding, M. C., R. Macdonald, J. E. Davies, and Fallick, A., E. (1993) Volatile characteristics of peralkaline rhyolites from Kenya: An ion microprobe, infrared spectroscopic and hydrogen isotope study, Contributions to Mineralogy and Petrology, 114, 264– 265.

Withers, A.C., and Behrens, H. (1999) Temperature induced changes in the NIR spectra of hydrous albitic and rhyolitic glasses between 300 and 100 K. Physics and Chemistry of Minerals, 27, 119–132.

Always consult and cite the final, published document. See http:/www.minsocam.org or GeoscienceWorld

Zhang, Y. (1994) Reaction kinetics, geospeedometry, and relaxation theory. Earth and Planetary Science Letters, 122, 373-391.

Zhang, Y., Stolper, E.M., and Ihinger, P.D. (1995) Kinetics of reaction H2O+O=2OH in rhyolitc glasses: Preliminary Results. American Mineralogist, 80, 593-612.

Zhang, Y., Belcher, R., Ihinger, P.D., Wang, L., Xu, Z., and Newman, S. (1997) New calibration of infrared measurement of dissolved water in rhyolitic glasses. Geochimica et Cosmochimica Acta, 61, 3089–3100.

Zhang, Y. (1999) H2O in rhyolitic glasses and melts: measurement, speciation, solubility, and diffusion. Reviews of Geophysics, 37 (4), 493-516.

Always consult and cite the final, published document. See http:/www.minsocam.org or GeoscienceWorld

DOI: https://doi.org/10.2138/am-2020-7363

Table 1 Composition of pantelleritic glasses (wt%).

Run#	SiO_2	Al_2O_3	MgO	CaO	FeO*	Na_2O	K_2O	Total
[a]0	76.60(1.02) **	8.55(0.46)	0.02(0.01)	0.23(0.05)	5.52 (0.21)	4.76(0.62)	3.71(0.41)	99.20
1	75.99(0.54)	8.34(0.18)	0.01(0.01)	0.25(0.03)	4.84(0.43)	6.79(0.10)	3.78(0.05)	98.14
2	76.85 (0.21)	8.28(0.17)	0.01(0.00)	0.26(0.01)	5.39(0.06)	5.45 (0.17)	3.76(0.40)	91.43
3	76.40(0.18)	8.34(0.06)	0.02(0.01)	0.25(0.02)	5.27(0.06)	5.97(0.17)	3.77(0.06)	93.46
4	75.62(0.53)	8.40(0.17)	0.01(0.01)	0.26(0.01)	5.50(0.17)	6.43(0.23)	3.78(0.05)	96.11
5	76.71(0.34)	8.25(0.10)	0.01(0.01)	0.26(0.02)	5.31(0.08)	5.77(0.15)	3.69(0.64)	92.39
6	75.45(1.91)	8.18(1.17)	0.01(0.00)	0.28(0.03)	5.83(1.01)	6.34(1.05)	3.89(0.39)	96.01
7	76.42(0.23)	8.53(0.11)	0.01(0.01)	0.26(0.02)	5.55(0.17)	5.49(0.71)	3.74(0.02)	92.53
9	76.66(0.54)	8.46(0.18)	0.02(0.01)	0.29(0.06)	5.42(0.08)	5.28 (0.62)	3.87(0.09)	91.65
10	76.33(0.42)	8.52(0.23)	0.01(0.00)	0.29(0.04)	5.18(0.13)	5.87(0.17)	3.81(0.09)	93.70
11	76.67(0.34)	8.46(0.12)	0.01(0.01)	0.29(0.04)	5.33(0.09)	5.36(0.25)	3.87(0.83)	91.96
12	75.83(0.38)	8.36(0.16)	0.02(0.01)	0.24(0.03)	5.44(0.28)	6.43(0.22)	3.69(0.11)	98.12
13	76.38(0.53)	8.32(0.11)	0.01(0.00)	0.26(0.03)	4.71(0.17)	6.58(0.27)	3.74(0.06)	96.20
14	76.30(0.50)	8.25(0.15)	0.01(0.00)	0.28(0.03)	4.42(0.37)	6.87(0.14)	3.87(0.04)	97.36

[a]Starting anhydrous composition. Individual oxide values are normalized to 100% total, while original total is reported in the last column.
* Total Fe as FeO.
**Values in parentheses are estimated standard deviations on 5-10 single analyses of glass samples.

Table 2 Experimental conditions and results of near-infrared spectroscopy and KFT analyses.

Run#	T (°C)	P MPa)	Quench	H_2O (wt% by KFT)	Density (g/L)	Thickness (cm)	(GG) A_{OH}	A_{H2O}	A^*_{OH} (cm^{-1})	A^*_{H2O} (cm^{-1})	(TT) A_{OH}	A_{H2O}	A^*_{OH} (cm^{-1})	A^*_{H2O} (cm^{-1})
1	850	150	SQ	1.09(0.09)	2368	0.0425	0.040	0.050	4.35	2.29	0.039	0.035	7.81	4.96
2	850	150	SQ	2.24(0.10)	2334	0.0394	0.068	0.095	6.70	6.77	0.070	0.095	13.92	12.63
3	850	150	SQ	3.75(0.09)	2291	0.0237	0.058	0.135	7.25	10.40	0.051	0.130	9.50	18.60
4	850	150	SQ	6.43(0.12)	2229	0.0534	0.130	0.500	15.03	37.30	0.115	0.503	21.26	71.71
5	850	150	SQ	6.25(0.13)	2223	0.0265	0.064	0.244	15.19	34.23	0.054	0.244	9.53	34.09
6	850	150	SQ	4.92(0.09)	2270	0.0060	0.012	0.048	2.20	7.27	0.013	0.049	1.88	6.73
7	850	150	SQ	6.53(0.10)	2220	0.0100	0.026	0.106	6.34	16.91	0.026	0.107	4.75	15.56
9	850	150	SQ	5.45(0.10)	2244	0.0360	0.085	0.330	9.97	23.79	0.073	0.335	12.76	47.18
10	850	150	SQ	4.48(0.09)	2271	0.0290	0.080	0.228	10.07	16.62	0.068	0.231	12.5	32.13
11	850	150	SQ	6.03(0.12)	2228	0.0148	0.040	0.156	4.78	11.81	0.035	0.156	6.02	21.80
12	900	30	FQ	1.93(0.08)	2325	0.1073	0.017	0.014	1.87	0.99	0.015	0.014	2.76	2.17
13	850	50	FQ	3.35(0.10)	2271	0.0763	0.016	0.028	1.66	2.08	0.016	0.030	3.16	4.44
14	850	50	SQ	3.24(0.09)	2271	0.1040	0.022	0.035	2.40	2.54	0.211	0.036	3.95	5.14

Absorbance and sample thickness are average of 3-5 spectra and measured values in different areas of the samples; error in thickness is 0.0002 cm. Densities are calculated based on Lange and Carmichael (1987) data. A_{OH} and A_{H2O} denote absorbance, A^*_{OH} and A^*_{H2O} integrated intensity. TT indicates that baseline is composed of a straight line, while GG of two Gaussians and a straight line (see text).

Table 3 Molar absorption coefficients for OH and H_2O combination bands for different hydrous glasses from literature

Composition	**τ [a]**	**SiO_2 (wt%)**	**Water range (wt%)**	**Baseline**	**ε_{OH} (L/mol·cm^{-1})**	**ε_{H2O} (L/mol·cm^{-1})**	**ε^*_{OH} (L/mol·cm^{-2})**	**ε^*_{H2O} (L/mol·cm^{-2})**	**Source of data**
Basalt	0.629	49.64	1.6-6.3	TT	0.56(5)	0.56(5)	123(26)	116(24)	Ohlhorst et al. (2001)
				GG	0.66(2)	0.65(2)	154(3)	143(3)	
MORB basalt	0.621	50.72	0.4-2.5	Five gaussians	0.67(3)	0.62(7)	-	-	Dixon et al. (1995)
Andesite	0.722	56.80	1.9-6.3	TT	0.68(2)	0.86(3)	135(8)	148(9)	Ohlhorst et al. (2001)
				GG	0.82(5)	1.01(7)	216(11)	153(8)	
Fe-Andesite	0.745	57.89	0.2-5.8	TT	0.79(7)	1.07(7)	-	-	Mandeville et al. (2002)
Fe-free Andesite	0.795	62.63	1.3-5.7	TT	0.89(7)	1.46(7)	-	-	
Dacite	0.782	65.19	1.5-5.9	TT	0.97(4)	1.11(5)	175(14)	188(15)	Ohlhorst et al. (2001)
				GG	1.12(3)	1.14(3)	252(11)	188(8)	
Pantellerite	0.853	76.60	1.1-6.5	TT	0.98(4)	1.92(2)	218(20)	245(23)	This study
				GG	1.00(4)	2.01(2)	229(40)	295(39)	
Rhyolite	0.856	77.04	1.0-6.2	TT	1.41(7)	1.66(5)	246(14)	238(8)	Withers e Behrens (1999)
				GG	1.52(8)	1.72(6)	310(17)	247(10)	

[a] $(Si^{4+}+Al^{3+})$/total cations; Error in the last decimal is given in parenthesis; for explanation on GG, TT and FC see text.

This is a preprint, the final version is subject to change, of the American Mineralogist (MSA)
Cite as Authors (Year) Title. American Mineralogist, in press.
DOI: https://doi.org/10.2138/am-2020-7363

Figure Captions

Figure 1 Near-infrared spectra of three pantelleritic glasses with total water content, ranging from 2.24 (0.10) wt% to 5.45 (0.10) wt% and sample thickness of 0.0394 to 0.0360 cm. Spectra offset vertically for clarity. In the spectra, the band at 4500 cm^{-1} is assigned to the combination of stretching and bending of OH group and the band at 5200 cm^{-1} to the combination of stretching and bending mode of H_2O molecules, while the 4000 cm^{-1} peak is unresolved (see the text).

Figure 2 Near-infrared spectrum showing baseline corrections. The original spectrum (RUN #3) shows the two peaks related to molecular water and OH groups at 5200 cm^{-1} and 4500 cm^{-1}, respectively, along with the band at ca. 3900-4000 cm^{-1}. a) Two (dashed) lines, which are tangential to the minima connecting the 4500- and the 5200 cm^{-1}-peaks, are illustrated to indicate the TT baseline correction procedure; b) the dashed line represents the GG baseline approach resulting from the combination of a gaussian plus a straight lines (see text for further details).

Figure 3 Normalized absorbances of the OH and H_2O-bands for pantelleritic glasses using TT and GG baselines and both evaluation methods of the absorption, peak height **(a)** and peak area **(b)**. Dashed and solid lines are linear regressions of the data fitted using a GG baseline and a TT baseline, respectively. The molar absorption coefficients for molecular water and OH group are given by intercepts on the y-and x-axes, respectively (see Table 3 and text for more details).

Figure 4 Measured concentrations of H_2O and OH versus total water content (c_{water}) in pantelleritic glasses determined using both the GG baseline and TT baseline and based on the evaluation of peak height **(a)** and peak area **(b)**. Note: H_2O speciation model curves from Dixon et al. (1995) compared with all data. At given total water content of the glass the relative amount of H_2O is almost equal within the errors if determined by using the peak height/area and GG/TT baseline procedure.

Figure 5 Total water content determined by Near-infrared spectra analysis versus water content measured by KFT. Note that there is a good correlation between the two sets of data determined by different methodologies, both in the case of the GG and TT baseline correction and evaluation of peak height and peak area. Both the 1:1 line and the four equations (and relative R^2 values) of the fit lines support the ability to fit the data with constant values of molar absorptivity (discussed further in text).

Always consult and cite the final, published document. See http:/www.minsocam.org or GeoscienceWorld

DOI: https://doi.org/10.2138/am-2020-7363

Figure 1

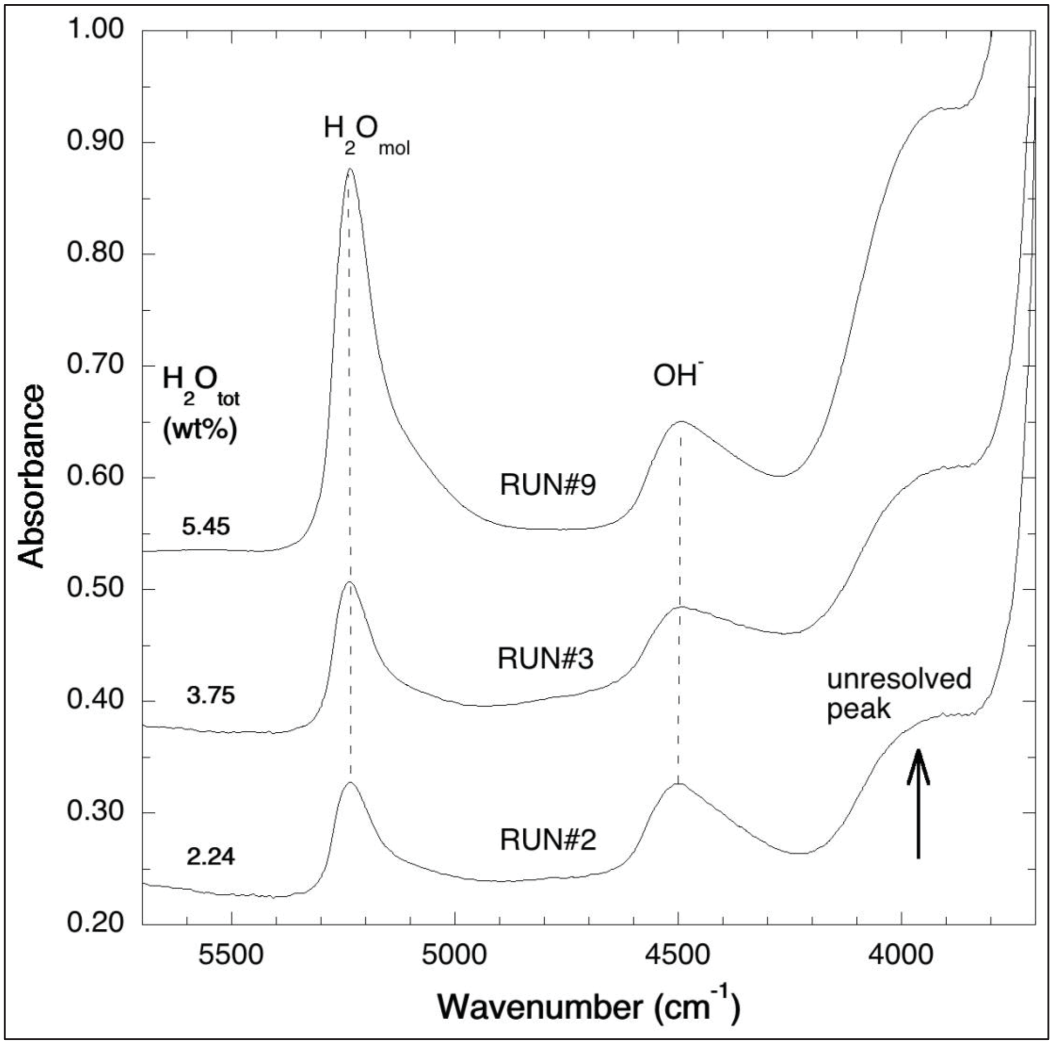

Figure 2

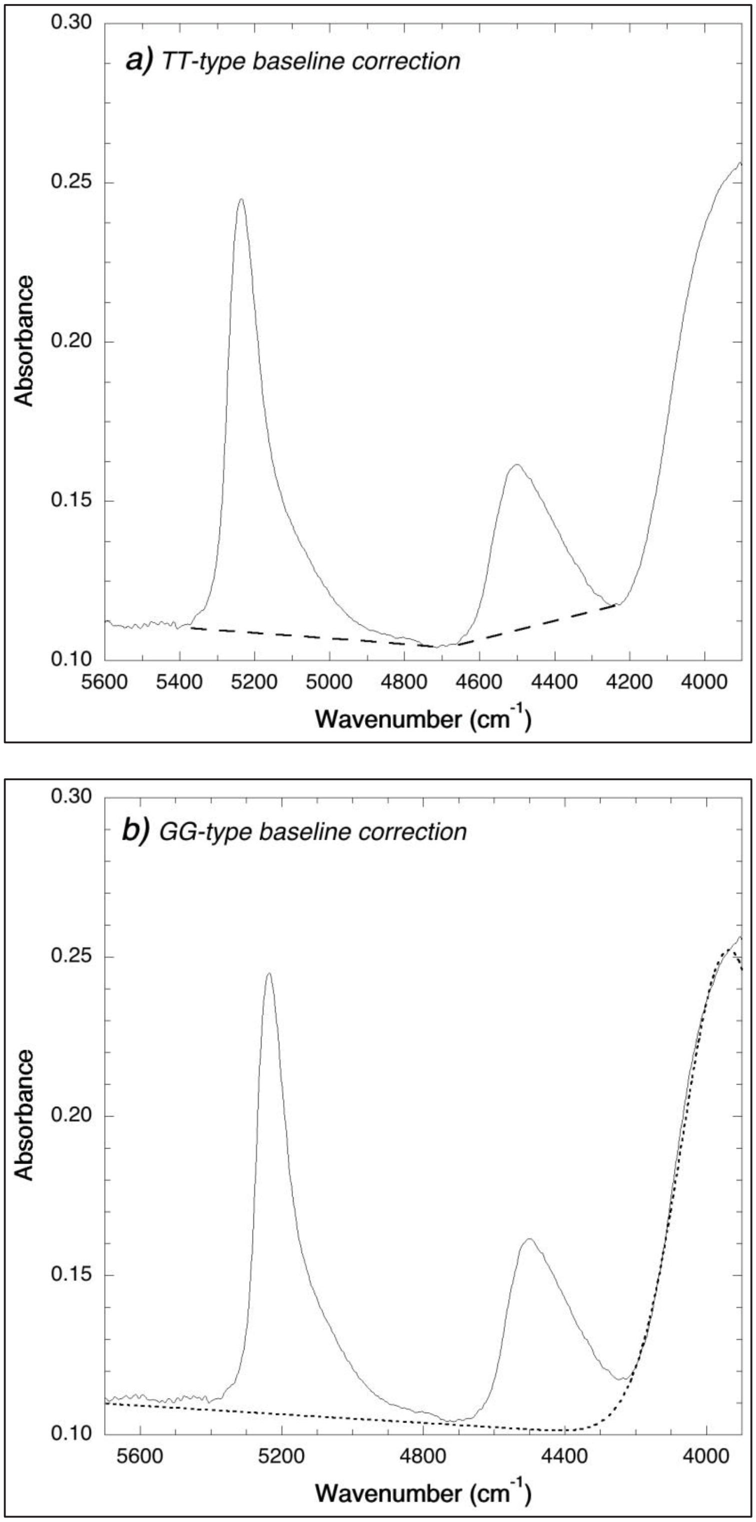

Always consult and cite the final, published document. See http:/www.minsocam.org or GeoscienceWorld

This is a preprint, the final version is subject to change, of the American Mineralogist (MSA)
Cite as Authors (Year) Title. American Mineralogist, in press.
DOI: https://doi.org/10.2138/am-2020-7363

Figure 3

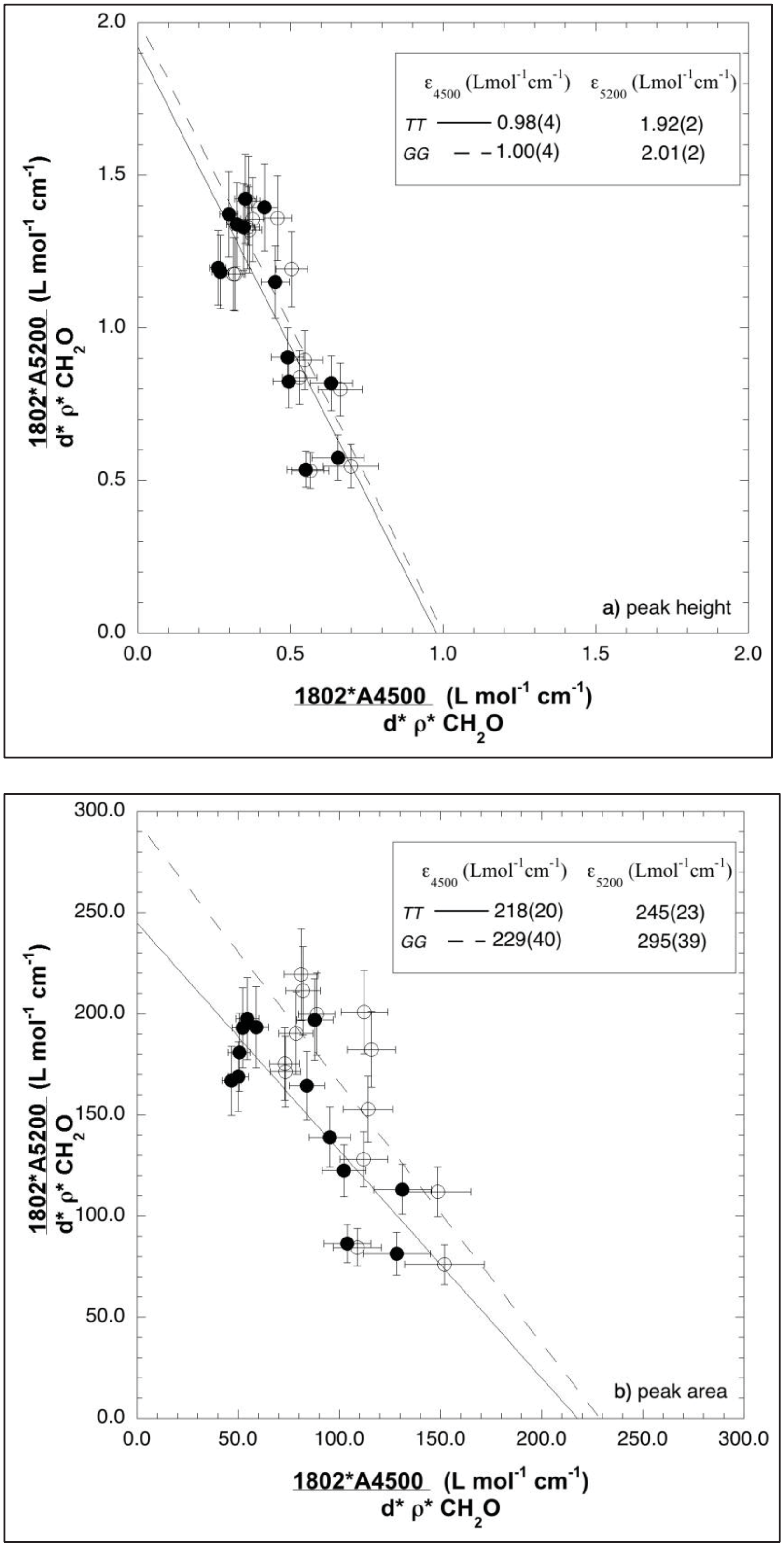

Always consult and cite the final, published document. See http:/www.minsocam.org or GeoscienceWorld

This is a preprint, the final version is subject to change, of the American Mineralogist (MSA)
Cite as Authors (Year) Title. American Mineralogist, in press.
DOI: https://doi.org/10.2138/am-2020-7363

Figure 4

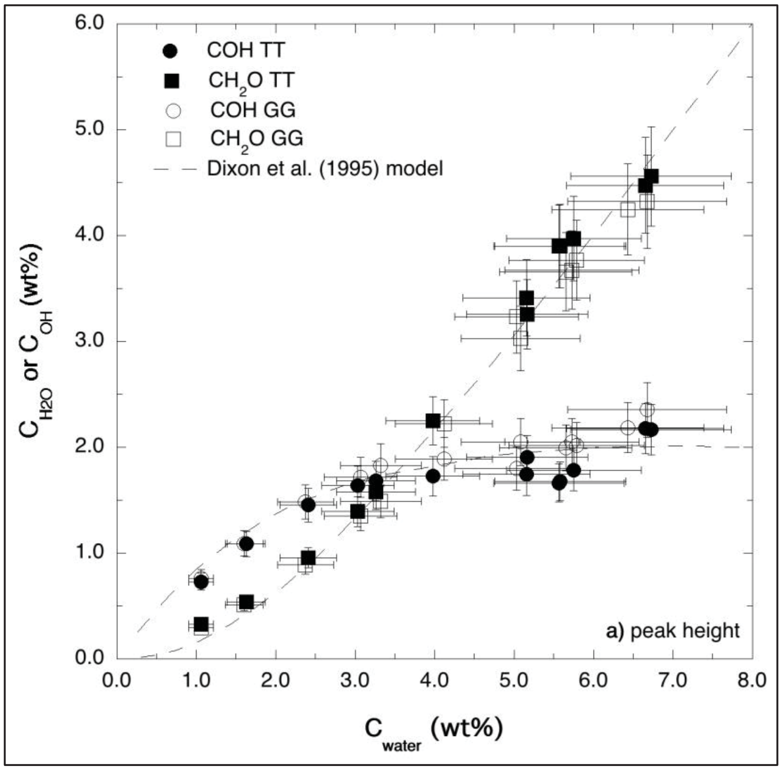

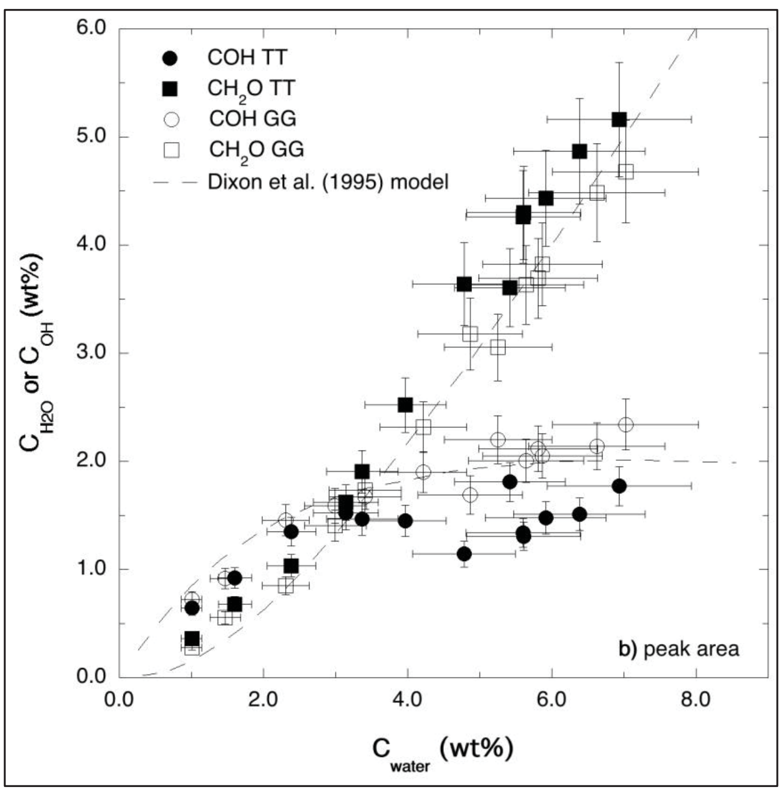

Always consult and cite the final, published document. See http:/www.minsocam.org or GeoscienceWorld

This is a preprint, the final version is subject to change, of the American Mineralogist (MSA)
Cite as Authors (Year) Title. American Mineralogist, in press.
DOI: https://doi.org/10.2138/am-2020-7363

Figure 5

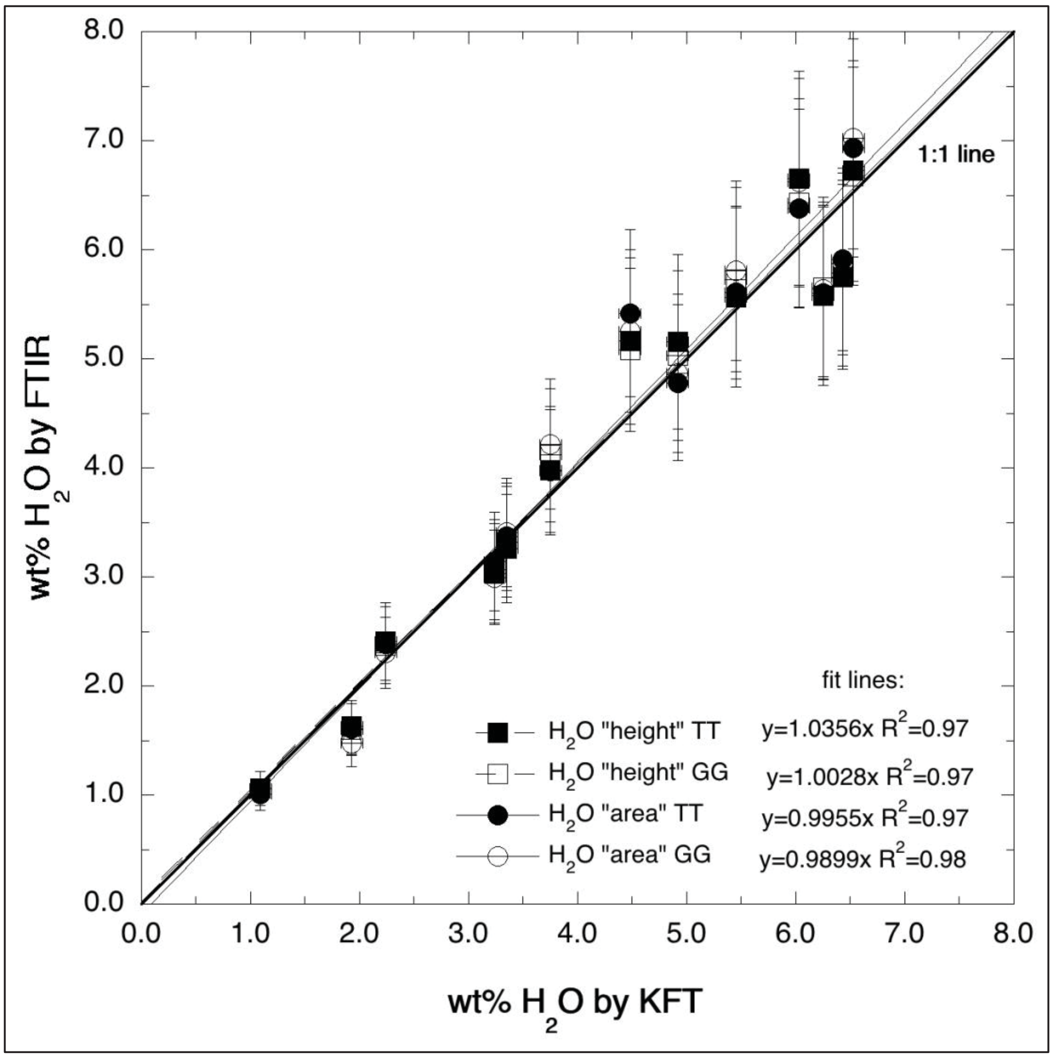

Always consult and cite the final, published document. See http:/www.minsocam.org or GeoscienceWorld